Self-Assembly of Crystalline−Coil Diblock Copolymer in Solvents with Varying Selectivity: From Spinodal-like Aggregates to Spheres, Cylinders, and Lamellae

Jun Fu,[†] Bin Luan,[‡] Xiang Yu,[‡] Yang Cong,[†] Jian Li,[†] Caiyuan Pan,[‡] Yanchun Han,*[,†] Yuming Yang,[†] and Binyao Li[†]

State Key Laboratory of Polymer Physics and Chemistry, Changchun Institute of Applied Chemistry, Chinese Academy of Sciences, 5625 Renmin Street, Changchun 130022, P. R. China, and Department of Material Science and Engineering, University of Science & Technology of China, Hefei 230026, P. R. China

Received September 25, 2003; Revised Manuscript Received November 25, 2003

ABSTRACT: We have investigated systematically the morphology of thin films spin-coated from solutions of a semicrystalline diblock copolymer, poly(L-lactic acid)-*block*-polystyrene (PLLA-*b*-PS), in solvents with varying selectivity. In neutral solvents (chloroform and tetrahydrofuran (THF)), a spinodal-like pattern was obtained and the pattern boundary was sharpened by diluting the solution. Meanwhile, loose spherical associates, together with larger aggregates composed of these associates by unimer bridges, formed partly due to crystallization of the PLLA blocks in relatively concentrated solutions. In slightly PS-selective solvent (e.g., benzene), both loose and compact spherical micelles were obtained, depending on the polymer concentration, coexisting with unimers. When enhancing the selectivity with mixed solvents, for example, mixing the neutral solvent and the slightly selective solvent with a highly PS-selective solvent, CS_2, loose assemblies (nanorods in CS_2/THF mixtures and polydisperse aggregates in CS_2/benzene mixtures) and well-developed lamellar micelles were obtained. For the lamellar micelles observed, a collapsed corona model is proposed to describe the geometry of dry platelets spin-coated on the substrates instead of the swollen coils in solutions.

1. Introduction

Block copolymers (BCs) are composed of covalently linked sequences of chemically distinct repeat units. In solvent selective for one of the blocks, micelles are usually formed with the insoluble cores and the soluble coronae when the concentration is well above the critical micelle concentration (cmc), as driven by incompatibility of the blocks and the precipitation of the insoluble blocks. The micellar structure has seen many fascinating applications such as coating, nanoreactor, encapsulation, and drug delivery. Increasing interest has recently arisen on BCs in selective solvents for both industrial and scientific significance.[1−4]

During the past decades, the micellar morphologies in dilute solutions have been extensively studied by static and dynamic light scattering methods,[5−11] small-angle X-ray (SAXS) and neutron scattering (SANS) techniques,[12−16] transmission electron microscopy (TEM),[17−20] and atomic force microscopy (AFM).[18] For block copolymers with wide composition range which have been studied to date, spheres are typically identified. The sphere size depends on the interplay of the solvent−core interface energy and the repulsion between the swollen corona chains. Micelle growth is favored by high surface tension between the core surface and the solvent in order to decrease the average area per chain. This results in an increase in the associate number of copolymers into a micelle and larger core volume. Consequently, the core chains will be highly stretched and the repulsion of the swollen corona chains increases. An entropy loss will thus arise as an oppose effect against the micelle growth. This problem can be resolved by reducing the micelle size or by a geometry transition from spheres to cylinders and vesicles or lamellae, where the chains in the cores become more relaxed. Such geometry transition has been observed by Zhang and Eisenberg[17] in the aqueous solutions of polystyrene-*b*-poly(acrylate acid) (PS-*b*-PAA) where the soluble PAA blocks are much shorter than the insoluble PS blocks. Similar sphere-to-rod transition was also reported[5] according to the analysis of the light scattering data for approximately symmetric block copolymers in selective solvents. The entropy loss is believed to induce such a transition.

We have been interested in the self-assembly of crystalline−coil block copolymers,[14−16,18−21] which contain at least one crystalline block. In highly selective solvents for flexible coils and precipitant to the crystalline blocks, the latter undergo chain folding to form crystal cores. Equilibrium lamellar geometry, as theoretically predicted[21] and experimentally observed,[14−16] contains a crystal core grafted with swollen corona at both surfaces. The repulsion between the swollen coils drives an increase in the fold number per chain so that the separation between the junctions of the blocks increases. This leads to thinner crystal platelets.[21] Flat layered structures have been investigated by SANS and SAXS.[14−16] Polyethylene (PE) and poly(ethylpropylene) (PEP) block copolymers[14−16] formed PE platelets grafted with hairy PEP coronae in PEP-selective solvents. The crystal layers varied from 3 to 8 nm thick. Moreover, with polymer fraction above a certain value, macroaggregates of these platelets were formed due to the very weak van der Waals interaction.[15]

Other self-assembled morphologies, including (star-like) spheres and cylinders, were inferred by Halperin

† Chinese Academy of Sciences.
‡ University of Science & Technology of China.
* Corresponding author: Fax +86-431-5262126; e-mail ychan@ciac.jl.cn.

10.1021/ma035447h CCC: $27.50
Published on Web 02/03/2004

et al.[21] as metastable state but recently reported by Winnik and co-workers,[18−20] who systematically studied the micelle formations of highly asymmetric crystalline−coil (with ratio as high as 1:12)[20] organometallic block copolymers. They extended their findings to wormlike, cylindrical, tubular, and spherical aggregates, depending on the copolymer composition and the micellization condition. Wormlike micelles, as argued by the authors to be driven and trapped by the crystalline cores, can extend to tens of micrometers or longer. Transition from cylinders to spheres occurred when the former was heated above the melting point (T_m) of the crystalline blocks. Similar properties were also found for nanotube-forming systems. These nonspherical aggregates, however, are rather stable over months.

These investigations on crystalline−coil assembly,[14−16,18−21] to our knowledge by far, have been exclusively conducted in highly coil-selective systems. The effects of solvent selectivity on the crystalline−coil copolymer micellization, however, have been less studied. This work is of interest in the effect of solvent selectivity, from neutral to selective, on the self-assembly of a crystalline−coil diblock copolymer.

For a given A-*b*-B diblock copolymer, a solvent can be classified as neutral (good solvent for both blocks), slightly selective (good for one but poor for the other), and highly selective (good for one block but nonsolvent for the other).[13,22−25] In general, neutral solvents can decrease the A/B interaction parameter (χ) by a factor of concentration (ϕ) in concentrated solution according to the dilute approximation proposed by Helfand and Tagami.[34] For dilute solution of neutral solvents, the effective A/B interaction parameter (χ_{eff}) should be much lower.[23−25,34] In other words, neutral solvents can shield the unfavorable contact of blocks. Therefore, the phase segregation strength is severely weakened. In a slightly A-selective solvent, the A blocks are swollen while the B blocks adopt a collapsed conformation.[13,22] In highly A-selective solvent, such swollen and collapsed conformations construct micelles. In short, variation of the solvent selectivity can shift the degree of microphase separation. For example, Eisenberg and co-workers[35] have finely controlled reversible transitions of various morphologies simply by manipulating solvent nature and composition. Similarly, the transition from spheres to cylinders, vesicles, and lamellae by changing composition of mixed solvents was also reported.[36]

This paper presents the effect of solvent selectivity on the self-assembly of a crystalline−coil diblock copolymer (PLLA-*b*-PS). From neutral to selective solvent conditions, a weakly segregated spinodal-like structure developed to micelle−unimer mixtures, polydisperse aggregates, and lamellar crystals.

2. Experiments

2.1. Block Copolymer Synthesis and Characterization. The diblock copolymer, poly(L-lactic acid)-*block*-polystyrene (PLLA-*b*-PS), was synthesized by combination of atom transfer radical polymerization (ATRP) and ring-opening polymerization (ROP). A hydroxyl-terminated PS synthesized by ATRP was used as the macroinitiator for following ROP of L-lactide monomers (Aldrich). The resulted PLLA-*b*-PS copolymer had number-average molecular weight (M_n) of 9400−10 400 with low polydispersity (<1.2), as determined by ^{1}H NMR and gel permeation chromatography (GPC). The synthesis details were described in ref 26. The volume fraction of the PLLA block is about 0.42, and this copolymer lies in strong segregation regime under present conditions.[27]

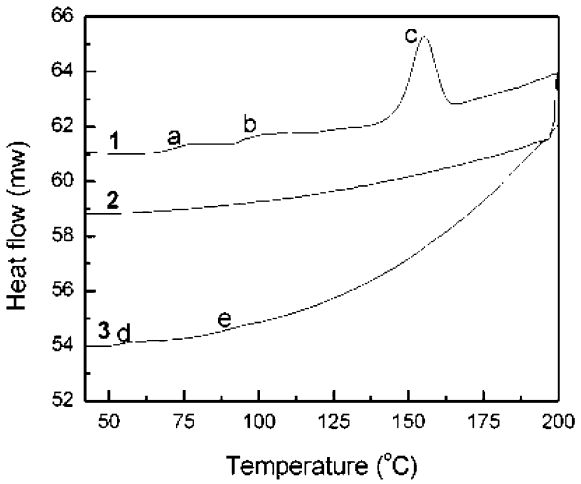

Figure 1. DSC curves of two heating and cooling runs at rate of 10 °C/min.

2.2. Differential Scanning Calorimetry (DSC). The thermal behavior of the PLLA-*b*-PS block copolymer was characterized with a Perkin-Elmer Diamond differential scanning calorimeter which has been calibrated before use. Two heating and cooling cycles were performed at rate of 10 °C/min within the temperature range from 40 to 200 °C, as shown in Figure 1. A 5 min stay was held after each heating and cooling. The first heating run saw two glass transitions at around 70 °C (a) and 95 °C (b) and an endothermic peak at 155 °C (curve 1). The glass transition temperatures (T_gs) are much closer to the bulk values of PLLA[28,29] and PS homopolymers.[30] The endotherm peak (c) can be accounted for the melting of PLLA block crystals, although it is lower than the bulk melting point (T_m) of homo-PLLA (*h*PLLA).[28,29] No exotherm was found at cooling (curve 2). The subsequent heating run produced two glass transitions at 55 (d) and 90 °C (e), lower than those of curve 1. The high-temperature endotherm was absent. This shift of the measured T_gs might be due to the change in thermal history of the powders.

From these results, it seems reasonable to infer that the PLLA-*b*-PS diblock copolymer powders were at a microphase-separated state.[29] The segregated domains individually behave as corresponding homopolymers. The PLLA block crystals confined within the PLLA-rich nanodomains melt at a lower T_m due to the finite size effect.[31] The absence of the crystallization and the melting upon cooling and the second heating run is similar to that reported in the literature.[32] This is because the crystallization of block copolymers is a thermodynamically controlled process, while the homopolymer crystallization is kinetically controlled.[21] This is not of interest here and will not be further discussed.

2.3. Sample Preparation. The PLLA-*b*-PS copolymer powders were dissolved into purified chloroform, tetrahydrofuran (THF), and benzene at room temperature. Storage over 24 h was used to obtain sufficient dissolution. For the THF and benzene solutions, the concentration was respectively varied. Finally, CS_2, a good solvent for PS[30] but nonsolvent for PLLA,[28] was added into the benzene and THF solutions drop by drop with oscillation. Slightly opaque bluish solutions were obtained when the weight ratios of benzene:CS_2 and THF:CS_2 approximately reached 2:1. All the solutions were spin-coated onto freshly cleaned silicon wafers with 2 nm native oxide cover. The residual solvent, which may influence the assembling or phase behavior, was immediately removed by drying in a vacuum oven at about 40 °C for more than 24 h.

2.4. Wide-Angle X-ray Diffraction (WAXD). The samples for WAXD characterization were prepared by casting the THF solutions of PLLA-*b*-PS copolymers onto glass slides. After the solvents evaporated spontaneously, a thorough removal of residual solvents was executed in a vacuum oven at 40 °C. WAXD spectra were obtained with a Rigaku D/max 2500 V PC X-ray diffractometer (Japan) with a Cu Kα source working at 40 kV and 200 mA.

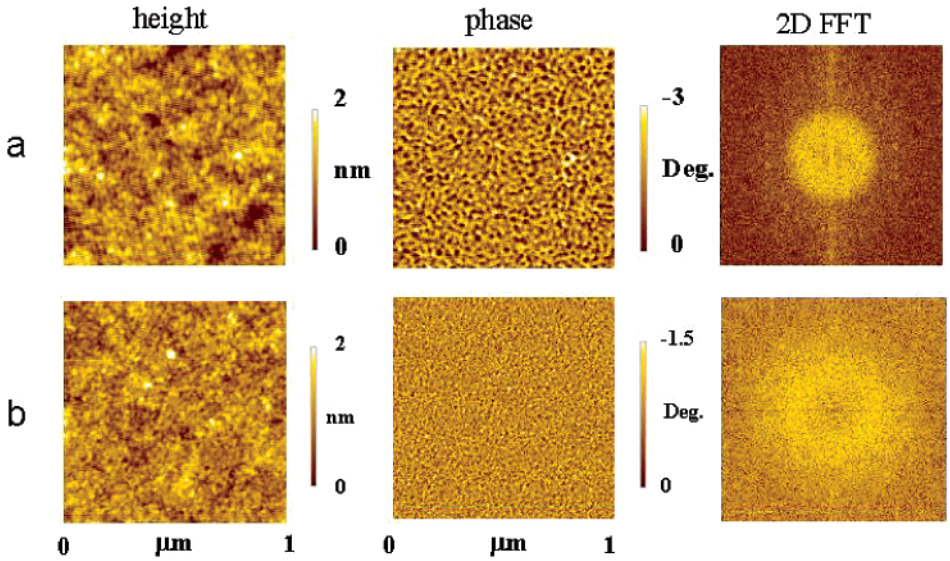

Figure 2. Tapping mode AFM images of films spin-coated from 0.5% (a) chloroform and (b) THF solutions. The left to right columns are height, phase images, and the corresponding 2D FFT patterns.

2.5. Atomic Force Microscopy (AFM). The surface morphology of all the films was characterized by a commercial atomic force microscope (SPA300HV/SPI3800N Probe Station, Seiko Instruments Inc., Japan) in tapping mode. The sample was mounted on a sample stage driven by a piezo tube scanner, which was calibrated with standard gratings before use. A silicon microcantilever (spring constant 2 N/m and resonance frequency ~70 kHz, Olympus Co., Japan) with an etched conical tip (radius of curvature ~40 nm as characterized by scanning over very sharp needle array, NT-MDT, Russia) was used for scan. The scan rate was ranged from 1.0 to 2.0 Hz to optimize the image quality. Each scan line contains 256 pixels, and a whole image is composed of 256 scan lines.

For acquisition of the surface morphology and material distribution, both topographical and phase images were recorded. Since both difference between the material mechanical properties and topographic fluctuation can contribute to the phase contrast,[33] the phase images were obtained under various conditions, including very fast and very slow scan, light, moderate, and hard tapping, and scan size from 20 μm to 500 nm, to ensure that the phase contrast pattern is mainly caused by mechanical reasons rather than topographic reasons. Only the representative phase images were chosen for discussion.

For the in-situ observation of the morphology evolution upon heating, a heat sample stage was mounted on the piezo tube scanner in a vacuum chamber. The temperature was controlled and monitored by thermal couples within ±1 °C error, as previously calibrated with standard gallium, indium, and tin samples. All analyses of the images were conducted at the software environment provided by the AFM manufacturer.

3. Results and Discussion

It is well-known that changing in solvent selectivity can shift the microphase separation of block copolymers, stabilizing the disordered state[22−25] or resulting in self-assembled structures from spherical micelles to cylinders, vesicles, and lamellae.[36] For a semicrystalline diblock copolymer in neutral solvents, the crystallization may contribute to the assembly, although the block incompatibility can be partly shielded by the solvent. The interplay between crystallization and the dissolution effect, as well as the segregation between the unlike blocks, will determine the aggregate morphology. By shifting the solvent condition, the assemblies will change their appearance.[35]

3.1. Spinodal-like Pattern at Film Surface from Nominally Neutral Solvents. 3.1.1. Morphologies from Neutral Solvents with Slightly Different Selectivity. Figure 2 compares the surface morphologies of the PLLA-*b*-PS films spin-coated from 0.5% (by weight as throughout the paper) chloroform (Figure 2a) and 0.5% THF (Figure 2b) solutions. The corresponding phase images (Figure 2, central column) clearly exhibit spinodal-like patterns. This is confirmed by the corresponding circular two-dimensional fast Fourier transform (2D FFT) pattern. In Figure 2a, the lateral (width) dimension of the fluctuating bumps is about 20 nm, very close to the microphase separation period (L) as measured from the strongly segregated relief structures (see section 3.3.1). From 0.5% THF solutions, the film surface is less fluctuating, and the corresponding phase contrast is low (Figure 2b), in comparison with Figure 2a.

Since tapping mode AFM scans over the same areas with different scanning rates and tapping forces produced almost the same spinodal-like patterns with the phase contrast less influenced,[33] one may take the light and dark regions as separated of PLLA and PS phases, respectively. The spinodal-like patterns indicate very weak microphase segregation of this very incompatible diblocks due to the shielding effect of solvents. Comparing the images in Figure 2a,b, one may conclude that chloroform is slightly more selective than THF is. In solutions of both solvents, the crystallization of the PLLA blocks is not seen since the strong solvation effect may prohibit chain folding.

3.1.2. Concentration Dependence of the Spinodal-like Patterns: Slight Increase of the Solvent Selectivity with Decreasing Concentration. When the solution concentration changed from 0.5% to 0.25% and 0.1% and even lower, the boundary of spinodal-like patterns became sharper (Figure 3). The surface fluctuating amplitude was remarkably enhanced from 2 to 3 and 5.5 nm, respectively (Figures 2b and 3). Correspondingly, the phase contrast increased with decreasing concentration. This trend in morphology evolution holds within the available concentration range below 1.0% (cf. section 3.1.3). A common feature of these patterns is that their lateral dimensions are around 20

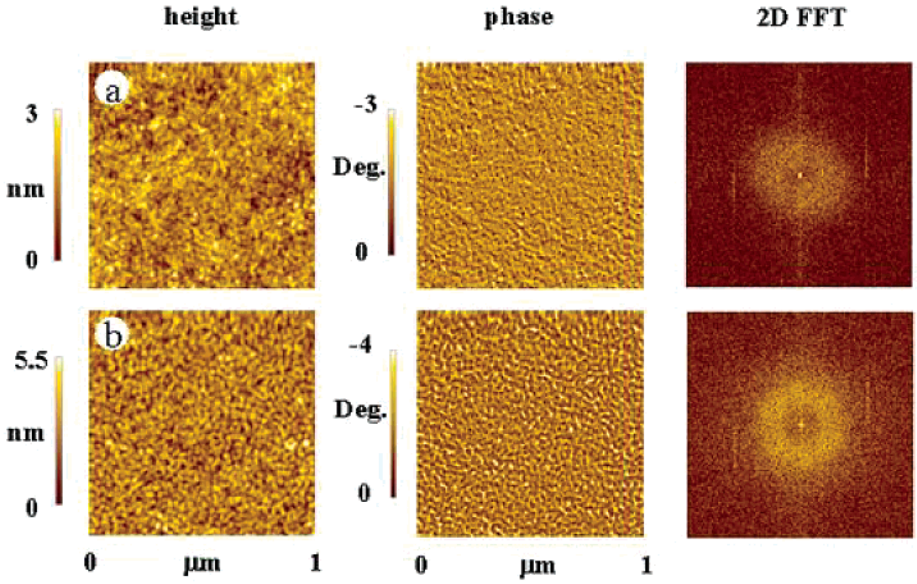

Figure 3. Typical surface morphology (left), phase image (central), and 2D FFT patterns (right) of films spin-coated from (a) 0.25% and (b) 0.1% THF solutions.

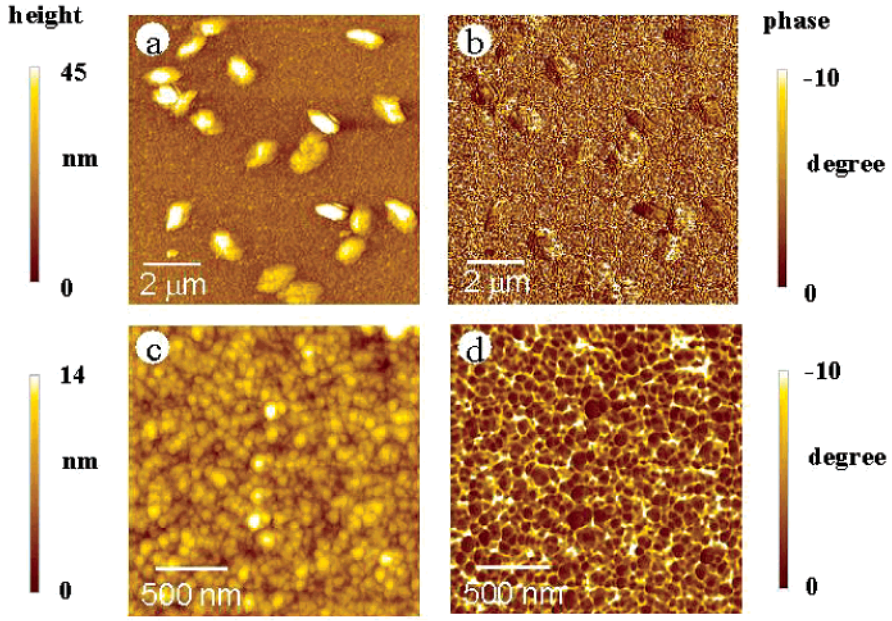

Figure 4. Spherical associates from 1.0% THF solutions: (a,c) height images; (b, d) phase images.

nm, very close to L (see section 3.3.1). The dependence of the spinodal-like pattern on concentration suggests that the phase segregation may be strengthened by lowering concentration.

This can be understood by considering the polymer−solvent interaction parameter (χ_{p-s}). Normally, the χ_{p-s} dependence on solution concentration could be positive, negative, or negligible.[30] THF is good solvent for PS and PLLA blocks, but the concentration dependence of the χ_{p-s} values for different polymer−solvent pairs usually differs from each other.[30] Thus, as concentration decreases, it is likely that the difference between χ_{THF-PS} and $\chi_{THF-PLLA}$ increases, leading to a slight shift in the solvent selectivity and a consequent increase in microphase separation strength of the blocks in solution. Remembering the dilution approximation,[34] however, one should not expect to reach the strong segregation regime only by infinitely diluting the solution by neutral solvent. But the situation seems totally different in the case of slightly selective system, as can be seen in section 3.3.

3.1.3. Crystallization-Induced Aggregates in THF. From relatively more concentrated THF solution (e.g., 1.0%), this PLLA-*b*-PS diblock copolymers associated into spherical aggregates, with diameter of several tens of nanometers (Figure 4). Some of these assemblies can even aggregate into larger grains (Figure 4a). The phase contrast is almost independent of the scan area, scanning rate, and tapping force. Therefore, it will be safe to take the dark domains as hard materials and the light domains as soft materials.[33] In relatively concentrated solutions, the PLLA blocks may crystallize, leading to aggregation of the polymer chains in the nominally neutral solvent, where the unaggregated copolymer chains (unimers) may serve as bridges connecting these associates into larger aggregates.[37]

The crystalline property of these aggregates was examined in situ by hot stage AFM in tapping mode

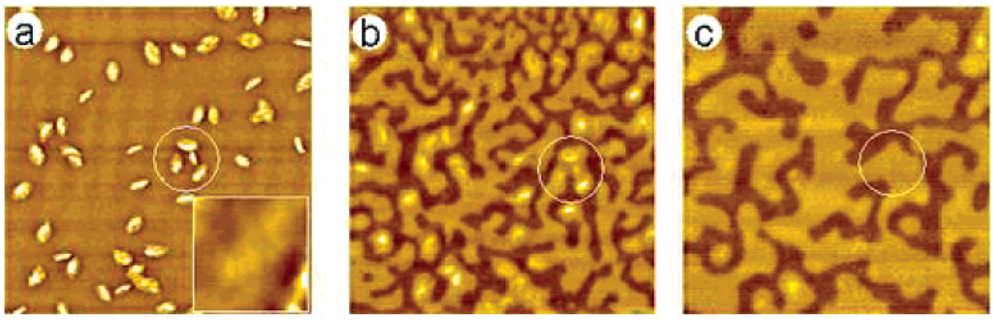

Figure 5. Morphology evolution upon heating the sample in Figure 4 from 20 °C to (a) 92 °C, (b) 155 °C, and (c) 169 °C. The scan areas are 20 × 20 μm^2.

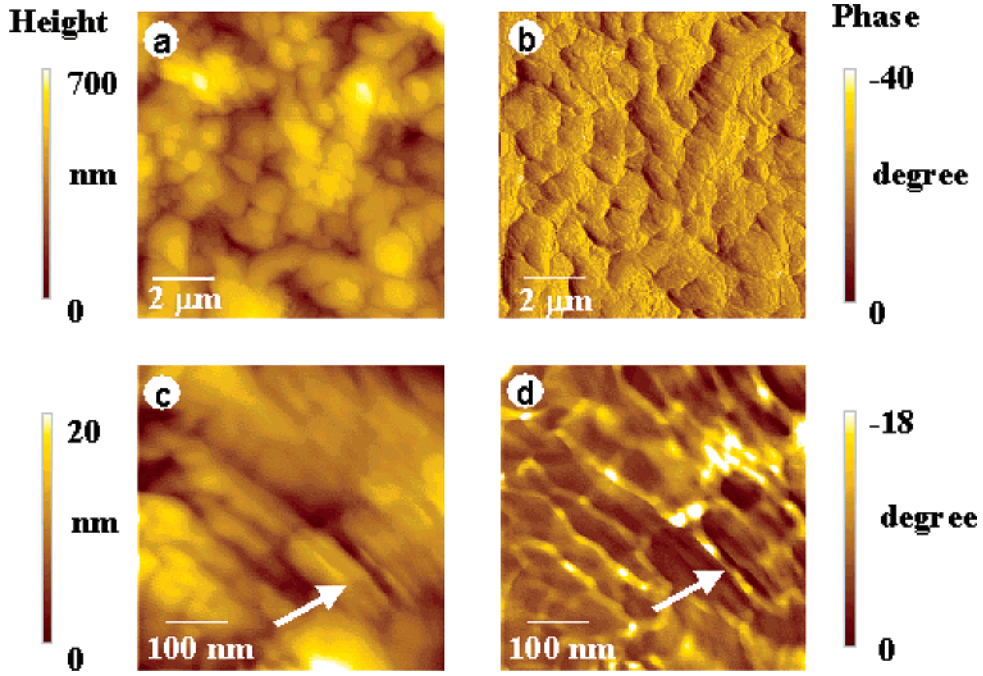

Figure 6. Surface morphology of films from 1.0% THF solution after spontaneous evaporation of the solvent: (a) spherulites; (c) the lamellae inside spherulite of 10 nm thickness; (b, d) phase images.

upon heating. A typical morphology evolution is shown in Figure 5. When the temperature approached the copolymer T_gs (e.g., 92 °C), the small aggregates became soft and flat (Figure 5a inset), but the larger ones remained their shape (Figure 5a), leading to drastic increase in phase contrast (not shown).[33] At $T_g \ll T < T_m$, microphase separation started and a bicontinuous pattern appeared (Figure 5b).[38] Yet, the large grains did not lose their shape until it reached the T_m of the PLLA blocks (155 °C), when several grains began to melt (Figure 5b). Thorough melting finally happened as the temperature reached 169 °C (Figure 5c), very close to the T_m of *h*PLLA.[28,29] As a result, a pseudo-bicontinuous relief structure with relative height of ~20 nm was obtained. This reveals the period of the microphase separation structure (L) of this PLLA-*b*-PS diblock copolymer.[38]

Upon heating, the small associates within larger ones converged, implying crystal growth. However, the large aggregates did not change their dimensions until melting started at T_m, indicating that they are isolated from neighboring small associates. The bridging copolymers permitted crystallization only inside the large aggregates. In contrast, the smaller aggregates without bridging copolymer chains could not grow; instead, softening happened at relatively low temperatures. These results indicate that the abnormal association of the crystalline−coil copolymer in a nominally neutral solvent may be largely attributed to the crystallization of the PLLA blocks. These associates may be loose rather than well-developed micelles for the strong solvation by THF.

This speculation was verified by evaporating the solvent spontaneously. The associates in 1.0% THF solution formed spherulite crystals (Figure 6a) that are composed of lamellar crystals (Figure 6c). These lamellae are ~10 nm thick and, according to the phase image (Figure 6d), separated from each other by light (in fact soft) spacing. The lamellar thickness is very close to that for *h*PLLA crystal platelets.[39] Remarkably, the phase contrast (18°) is much higher than those in Figure 4, indicating better crystalline structures may form. The WAXD spectrum confirmed the crystalline structure of the layers. As shown in Figure 7, the most intensive scattering peak at $2\theta = 16.84°$ indicates a spacing of 5.26 Å. This value is much close to the crystal lattice spacing (5.17 ± 0.08 Å) of the *h*PLLA lamellar crystals from *p*-xylene solutions.[39]

3.2. Coexistence of Spherical Micelles and Unimers in a Slightly Selective Solvent, Benzene. In benzene, a slightly PS-selective solvent, micellization occurred. Figure 8 presents typical results from PLLA-

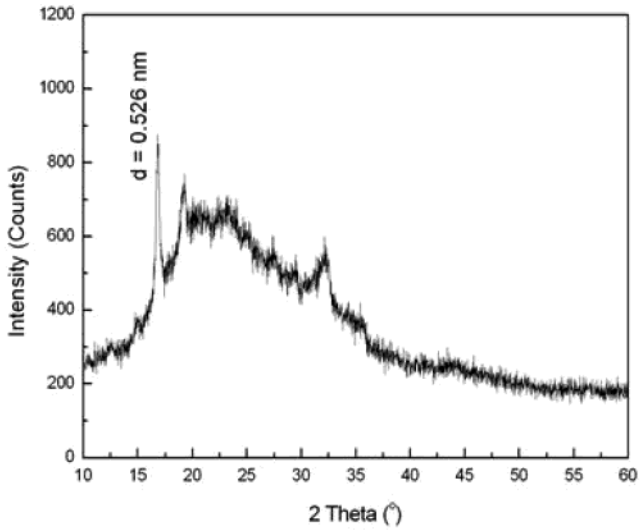

Figure 7. WAXD spectrum of the copolymer film by casting 1.0% THF solution onto glass slide.

b-PS/benzene solutions with different solution concentrations. Figure 8a−d presents the height and phase images for films spin-coated from 2.0% and 0.5% benzene solutions. Spherical micelles are found accompanied by low phase contrast. The decrease in concentration leads to slight increase in micellar size and phase contrast. The poor phase contrast implies that the micelles are loose associates. When the temperature was elevated to 30 °C and higher, the micelles disappeared, indicating that benzene became neutral at high temperatures.[28,30]

It is interesting to find that the micelles from 0.1% solutions gave rise to much higher phase contrast (∼20°) between the core and the corona (Figure 8e,f). From the images of 500 × 500 nm^2 area (insets), the interface between the core and corona is rather sharp and almost independent of the scanning rate, tapping force, and scan area. The phase contrast is much close to the phase contrast in Figure 6d. This implies that the micelle cores may be crystalline, in which the PLLA blocks fold.[21] The PS blocks extend from the crystal surface into solutions.

We have been aware of the concentration dependence of the solvent selectivity in section 3.1.2. The transition from loose micelles to crystal core micelles seems to some extent supporting this argument. Such micelles with crystal cores are somewhat analogous to the starlike micelles proposed by Vilgis and Halperin.[21] According to the scaling theory analysis, the authors argued that the starlike micelles are metastable. However, the micelles obtained here are rather stable over at least 6 months. Consideration of this micellar formation according to Halperin's scaling theory will be discussed in section 3.3.3.

3.3. Nanorods, Polydisperse Aggregates, and Lamellar Crystals Formed by Addition of Highly PS Selective Solvent. Addition of a precipitant to one

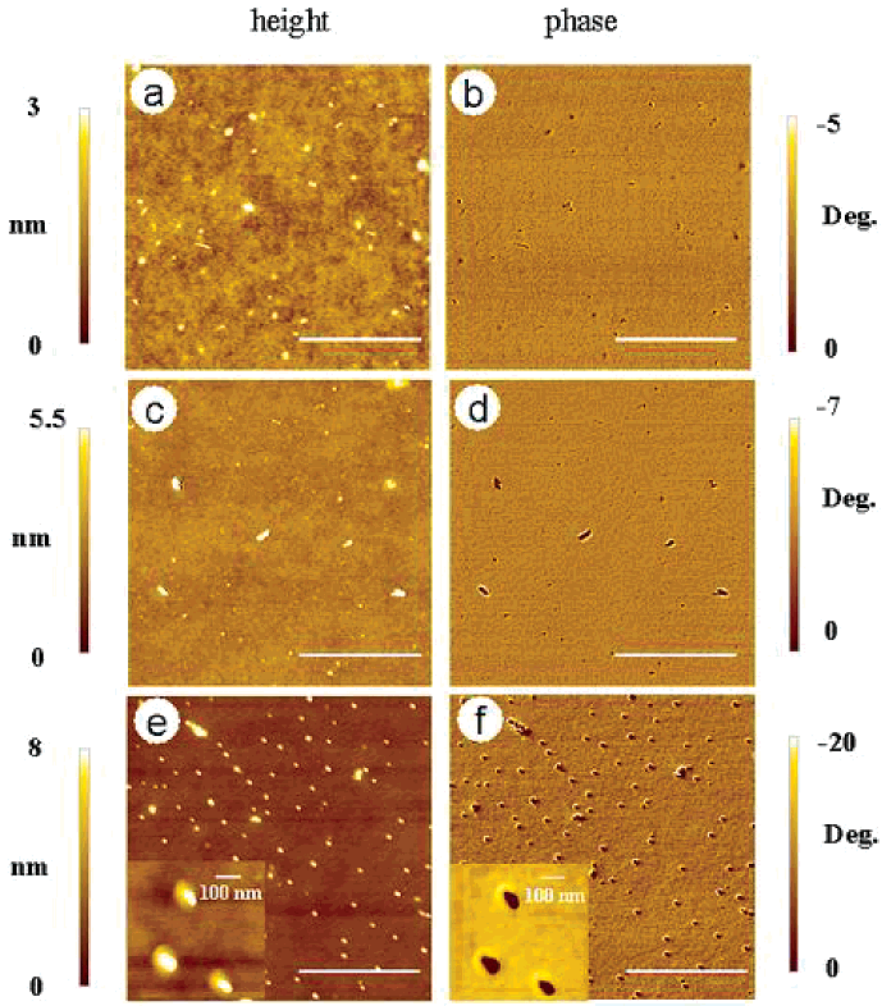

Figure 8. AFM height and phase images of spherical micelles from (a, b) 2.0%, (c, d) 0.5%, and (e, f) 0.1% benzene solutions. The scale bars represent 2 μm.

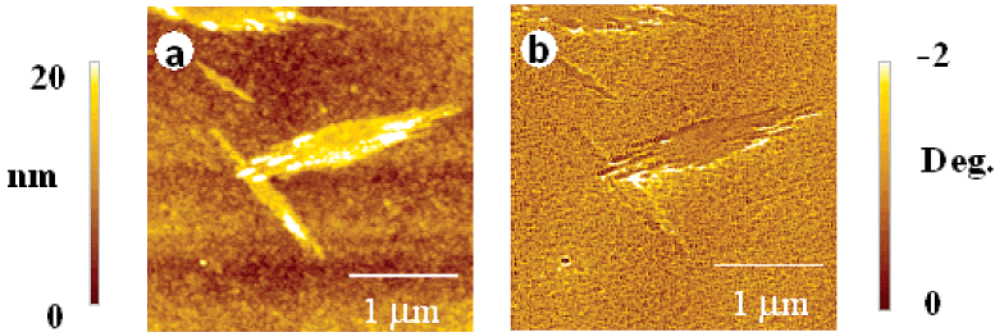

Figure 9. Typical AFM height (a) and phase images (b) of bundles of nanorods.

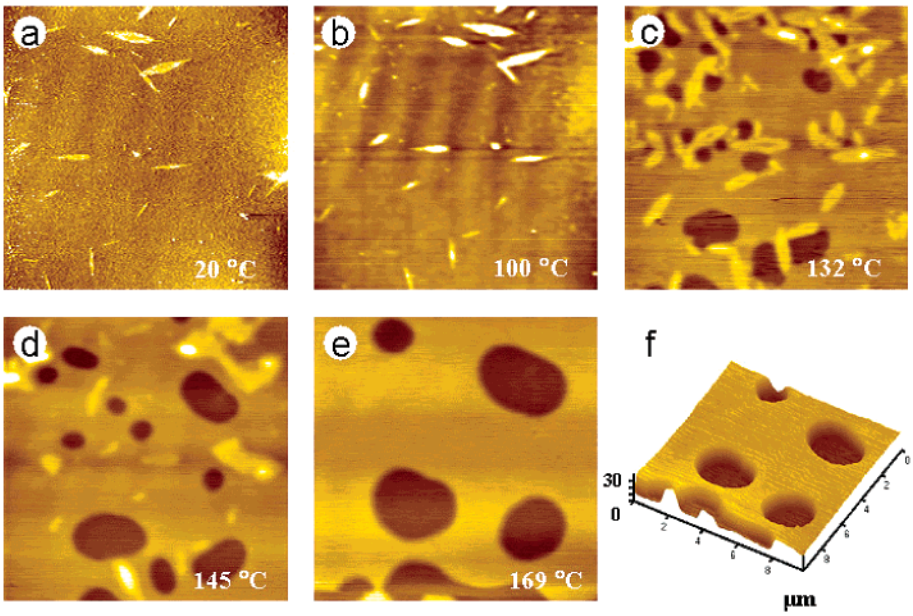

Figure 10. (a) Rodlike assemblies from 1.0% THF solution with addition of CS_2 (about 2:1). (b−e) In-situ AFM observation of the morphology evolution upon heating.

of the blocks has been widely used to promote solvent selectivity. With different composition of solvent/nonsolvent mixture, block copolymer aggregates can largely differ from micelles, cylinders, and vesicles.[35,36] Here, CS_2, a good solvent for PS but precipitant for PLLA blocks, was slowly added into both solutions in neutral THF and slightly selective benzene. New aggregates are obtained.

3.3.1. Bundles of Nanorods Rodlike structures were formed with addition of CS_2 into 1.0% THF solutions (Figure 9). These nanorods are polydisperse in both geometry and size. Their diameters varied from ~20 to 50 nm and the length extended to as long as 2 μm. These nanorods showed a liability to form bundles. Although topographic fluctuation is obvious, the phase image is rather ambiguous (Figure 9b). It is hard to distinguish the boundary between the rods integrated into the bundles. This indicates that they may interconnect each other. Moreover, the edges of the rods are hairy, which is especially apparent from the phase contrast. This feature is much different from the cylinders, as widely reported, in which well-developed core−corona structures are identified.[18−20] These facts lead to a speculation of homogeneous material distribution throughout the aggregates.

It is known from section 3.1.3 that there are loose spherical associates driven by crystallization in 1.0% THF solution. The addition of CS_2, which is fairly soluble in THF, has effects of increasing the interfacial energy between the solvent and the PLLA blocks. Besides, it competes with the copolymers for the dissolution of THF. Thus, the solvent quality becomes poor. (Indeed, if the content of CS_2 is high enough, copolymers will precipitate.) Similar thermodynamic alternations in solution condition for coil−coil block copolymers normally lead to transitions from spheres to cylinders with insoluble cores and swollen coronal, leading to a radical density gradient of the blocks.[14−16,18−21,35] In our case of semicrystalline block copolymers, the crystallization of the blocks may kinetically prevent the formation of such normal cylindrical micelles. Instead, the homogeneous material distribution may root from the strong solvation effect of THF on both blocks, and these cylinders might be loose.

This seems verified by in-situ observation of the evolution of these nanorods by hot stage AFM scan (Figure 10). As temperature increased, the rods were softened and began to grow at 100 °C (Figure 10b). Such growth of the rods expends the neighboring materials, leading to material depletion around the rods so that holes emerged at 132 °C (Figure 10c). As temperature reached 145 °C, many of the grown rods began to melt and the material flowed back to eliminate some holes (Figure 10d) until all the rods melted at 169 °C (Figure 10e). This melting behavior is much similar to that of the bulk, indicating that, during heating, crystals were

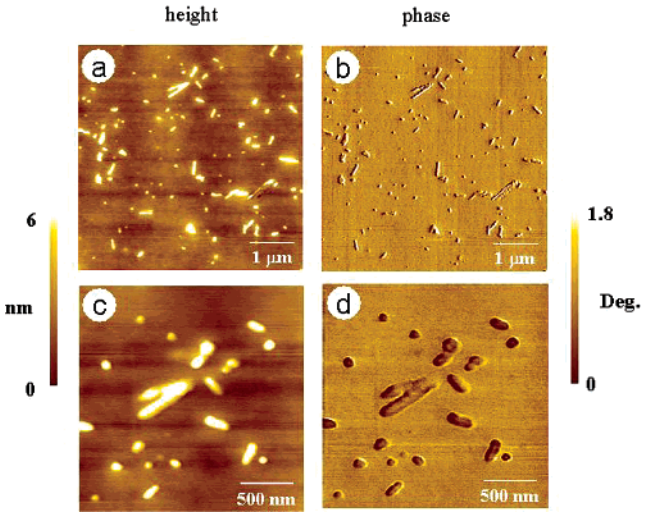

Figure 11. Polydisperse assemblies from 1.0% benzene solution with addition of CS_2 in ratio of about 2:1. Aggregates of spheres, ellipsoids, and cylinders are obtained.

developed within the growing nanorods. The growth of the rods and depletion of adjacent copolymers indicates that the rods are partly crystalline and open. At molten state, holes are formed with depth of ca. 20 nm, equal to L (Figure 10f).[38]

3.3.2. Polydisperse Aggregates. By slow addition of CS_2 into 1.0% benzene solution, opaque solutions were obtained. Figure 11 displays a typical surface morphology of film spin-coated from these solutions. Spherical, ellipsoidal, and rodlike aggregates are observed. From the height images, it is seen that the dimensions of the aggregates are larger than L and the micelle size from benzene solutions (Figure 8). From corresponding phase images, very low phase contrast was found, almost independent of the scanning conditions. This poor phase contrast, in comparison with that for crystalline structures, indicates that no crystals are formed. The dilation in lateral dimension may root from the swelling of the core by the solvent.

In mixed solvents, earlier light scattering studies by Kurata and co-workers[5] found the existence of ellipsoidal micelles of PS−PMMA diblock copolymer with axial ratio of ∼3.9 within narrow solvent composition range. Zhou and Chu have observed abnormal association of a triblock copolymer of poly(ethylene oxide) and polystyrene, PEO−PS−PEO, at some intermediate temperature range.[6] But they attributed this abnormal micelle formation to the composition polydispersity rather than the inherent property of the block copolymer itself. Recently, PS−PMMA diblock copolymer in mixed selective solvents of benzene/*p*-cymene formed loosely associated regular micelles under the weak segregation condition.[10] In slightly PS-selective solvent, block copolymers of polystyrene and polyisoprene[13,24] formed micellar structures that can be described by model form factors of ellipsoidal and cylindrical micelles. These micelles are polydisperse, in both size and shape. Essentially, the changes in solvents or composition for mixed solvents mean changes in solvent quality.[9,12] Better solvent condition favors a decrease in aggregation number into micelles, and worse solvent condition induces larger aggregation. For triblock copolymer of PEO and poly(propylene oxide) (PPO), PEO−PPO−PEO, in aqueous solution, if the additional cosolvent (e.g., glycerol) competes with the PPO block for water solvation, the micelle formation is promoted.[12]

In our work, the addition of CS_2 will undoubtedly compete with PLLA blocks for the benzene solvation. (CS_2 droplets can precipitate from the benzene solution at some critical content.) Therefore, the solvent quality becomes worse with addition of CS_2 and the micelles grow, even together with transitions from spheres to ellipsoids and cylinders. The PLLA blocks did not crystallize due to the strong swelling effect of benzene. However, the situation changed as we added nearly the same amount of CS_2 into the solution of micelles with crystalline cores, as given in the following section.

3.3.3. Lamellar Micelles. It is interesting to find that, with addition of CS_2 into 0.1% benzene solutions, lamellae emerged (Figure 12). These well-developed platelets appeared as either single layer or bilayer, with thickness of ∼8 nm according to the AFM height images and the corresponding cross-section line scan profile. It is clear that some of these polygon lamellae have angles of 120°. This may imply that the PLLA blocks fold hexagonally to form crystal cores.[39,40] However, these crystals are far from the perfect hexagonal single crystals of *h*PLLA[39,40] since the thermodynamic constraint is somewhat dominant. The surface is in no way flat since the coil blocks grafted at the crystal surface. Frequently, we encounter basinlike lamellae of which the edges are 1−2 nm thicker than the center because there is less repulsion at the edges.

To understand the formation of spherical (Figure 8e,f) and lamellar micelles with crystal cores, the scaling analysis by Vilgis and Halperin[21] is considered here. A crystalline−coil A−B diblock copolymer associates in highly B-selective solvent, forming micelles with crystal cores and swollen coronae. The (N_A) crystalline A block undergoes tight folding in adjacent reentry mode (Figure 13). The micellar geometry is a balance between the interfacial energy between the solvent and the core surface and the repulsion between the swollen coils. The minimization of the core−solvent interfacial energy favors a decrease in the surface area per chain, which results in an increase in associate number, f, into a micelle. Consequently, the repulsion between the swollen coils increases and the coil chains are more stretched. Such strong repulsion leads to a large number of chain folds, n_f, and small lamellar thickness, l.

The surface energy of the anisotropic crystalline cores, much different from that of the isotropic coil micelle cores, involves two surface tensions: the surface tensions of the lateral surface (σ_l) and the fold surface (σ_f), as schemed in Figure 13. A general form for the surface free energy per chain, $F_{surface}$, is given by

$$\frac{F_{surface}}{kT} \approx n_f \frac{\sigma_f a^2}{kT} + \frac{S_{lateral}\sigma_l}{fkT} \qquad (1)$$

where k is the Boltzmann constant, a is the monomer size, $S_{lateral}$ is the lateral surface area of the core, and T is temperature. For starlike micelles, $S_{lateral} \approx N_A f^{1/2} n_f^{-1/2} a^2$. Thus, $F_{surface}$ reads

$$\frac{F_{surface}}{kT} \approx n_f \frac{\sigma_f a^2}{kT} + N_A f^{-1/2} n_f^{-1/2} \frac{a^2 \sigma_l}{kT} \qquad (2)$$

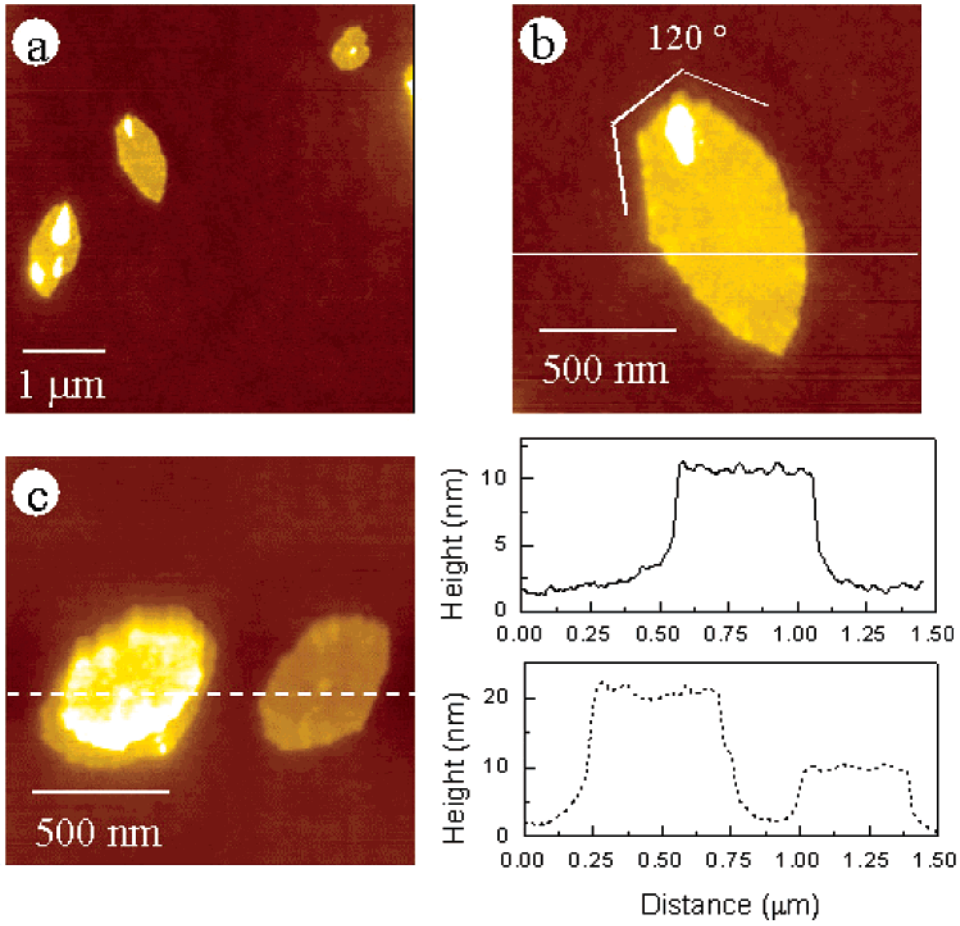

Figure 12. Lamellar aggregates formed from 0.1% benzene solution with addition of CS_2 in ratio of about 2:1. Both single-layer (b) and bilayer lamellae (c) are found. The cross-section line scan profiles give out the lamellar thickness ~ 8 nm.

Combining $F_{surface}$ with the coronal free energy of the starlike micelles, $F_{corona}/kT \approx f^{1/2}$, the micelle free energy is given by

$$\frac{F}{kT} \approx f^{1/2} + n_f \frac{\sigma_f a^2}{kT} + N_A f^{-1/2} n_f^{-1/2} \frac{a^2 \sigma_l}{kT} \qquad (3)$$

The equilibrium micellar size can be yielded as

$$l \approx N_A^{3/5} \left(\frac{kT}{\sigma_l a^2}\right)^{2/5} \left(\frac{\sigma_f a^2}{kT}\right)^{4/5} a \qquad (4)$$

$$D \approx N_A^{1/5} \left(\frac{\sigma_l a^2}{kT}\right)^{1/5} \left(\frac{kT}{\sigma_f a^2}\right)^{2/5} a \qquad (5)$$

$$R_{core} \approx N_A^{3/5} \left(\frac{\sigma_l a^2}{kT}\right)^{3/5} \left(\frac{kT}{\sigma_f a^2}\right)^{1/5} \qquad (6)$$

and the equilibrium free energy is given by

$$F/kT \approx N_A^{2/5} \left(\frac{\sigma_l a^2}{kT}\right)^{2/5} \left(\frac{\sigma_f a^2}{kT}\right)^{1/5} \qquad (7)$$

Here, D is the average distance between the grafting sites or the lateral dimension of a single chain in the fold surface. The micelle core is shaped as $R_{core}/l \approx \sigma_l/\sigma_f$. Therefore, for a moderate σ_l/σ_f value, the overall micellar geometry appears as spherical, while for larger σ_l/σ_f values, highly core anisotropy is expected. In both situations, the crystalline blocks within the cores adopt anisotropic configuration.

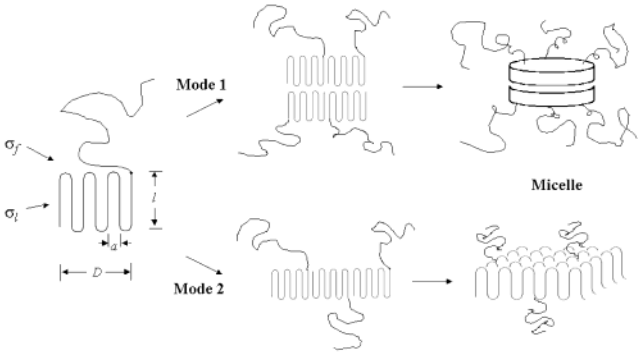

Figure 13. Schematic drawing of the formation of spherical (mode 1) and lamellar micelles (mode 2).

For lamellar micelles, the surface energy per chain is

$$\frac{F_{surface}}{kT} \approx n_f \frac{\sigma_f a^2}{kT} + N_A n_f^{-1/2} \frac{a^2 \sigma_l}{kT} \qquad (8)$$

At equilibrium state, the surface free energy

$$\frac{F_{surface}}{kT} = N_A^{2/3} \frac{\sigma_l^{2/3} \sigma_f^{1/3} a^2}{kT} \qquad (9)$$

The lamella free energy is given by

$$F/kT \approx N_B^{6/11}\left(\frac{\sigma_f a^2}{kT}\right)^{5/11} \quad (10)$$

In this case, only σ_f contributes to F and σ_l has no influence on F. Though, the anisotropy of a single folding block D/l is determined by σ_l/σ_f. Therefore, when σ_l is much larger than σ_f, a crystalline block will form a large number of folds to produce highly anisotropic configuration ($D \gg l$).

As the surface tension contribution to the sphere-to-lamella transition is concerned, it is intuitive to compare, at least qualitatively, the interfacial energy between the PLLA core and the solvents. To this end, we arbitrarily compared the droplet shape of benzene and CS_2 on *h*PLLA crystal surface. Benzene spread rapidly on the PLLA surface whereas a collapsed CS_2 droplet formed. Both solvents evaporate rapidly, which makes it hard to accurately determine the contact angle of these droplets on PLLA sheets. This arbitrary comparison indicates that the interfacial energy between the CS_2 and PLLA core surface is larger than that between the benzene and PLLA core surface. With addition of CS_2, the interfacial energy at the crystalline PLLA core surface is enhanced. It is likely that such increase in interfacial energy may have a much larger effect on σ_l than on σ_f.[20] Therefore, a lamellar geometry (mode 2 in Figure 13) of which the surface energy is independent of σ_f seems favorable (eq 10). From eqs 4−6, the increase in interfacial energy will largely increase the anisotropy of a single PLLA block and the cores since $R_{core}/l \approx \sigma_l/\sigma_f$ and $D/l \propto \sigma_l^{3/5}/\sigma_f^{6/5}$. The number of chain folds will increase, and the micelles (mode 1 in Figure 13) will extend laterally. On the other hand, the increase in $F_{surface}$ requires micelle growth by incorporation more copolymer chains. Such micelle growth leads to a decrease in core curvature since the chain folds within the core extends laterally in plane. That is, lamellae are favored. Since CS_2 is a good solvent for PS, the coronae will be more swollen. Chain repulsion leads to more stretching of corona chains. The corresponding free energy penalty of coronae requires the increment of the fold number per chain (n_f) to relax the chain stretching. As a result, the platelets become thinner.

The micellar platelets appeared as a crystal core grafted with solvent-swollen coronae at both sides.[14−16] The lamellar thickness (t) is a sum of the corona thickness (H) and the core thickness (l), i.e., $t = 2H + l$. In this work, $t \approx 8$ nm and the gyration radius of the unperturbed PS block, R_g, is about 3 nm.[24] Assuming a Gaussian conformation (Figure 14a) for the PS chains in solution, $2H \approx 2{\cdot}2R_g = 12$ nm > t. This might contain an implication that, for the platelets observed here, the PS coronae adopt a severely collapsed conformation (Figure 14b) in comparison with the stretched and swollen one in solutions.[14−16]

When the solvent evaporates and the dry platelets are exposed to air, the PS blocks are likely to assume a collapsed conformation due to the confinement effect[41] as well as minimization of the surface free energy by covering the surface with low-surface-energy PS blocks. Assuming that the collapse ratio of the PS coils is as large as 60%,[41] i.e., the surface corona thickness is about 2.4 nm, thus the crystal core thickness approximates 3 nm according to the sandwich model. In fact, because of the strong incompatibility between the PS and PLLA blocks and the repulsion between the PS coils in solution, the 60% collapse (proposed for the PS chains confined at thin PS film surface) seems overestimated, and a less collapse ratio (e.g., 50% or less) is more reasonable. Therefore, the crystal lamellar core should be thinner than 3 nm.

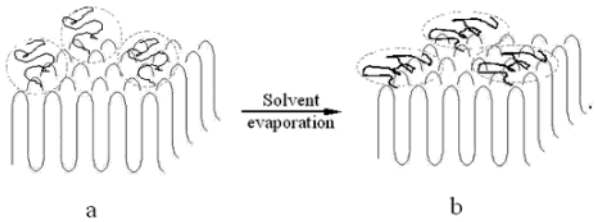

Figure 14. Schematic illustration of a transition of the swollen coronal conformation in solution (a) to the proposed collapsed conformation (b) after removal of solvents. The lamella is grafted by the flexible coils at both sides, whereas only one side is schemed for simplicity.

4. Conclusions

The self-assembly of a semicrystalline PLLA-*b*-PS diblock copolymer in neutral, slight selective, and highly selective solvents is investigated. In nominally neutral solvents, i.e., chloroform and THF, weak segregation happened to produce spinodal-like patterns with lateral dimension of ∼20 nm (L). The segregation strength increased with decreasing solution concentration.

In relatively more concentrated THF solutions (e.g., 1.0%), crystallization of the PLLA blocks induced loose spherical associates of the copolymers, although perfect crystallization is prohibited by the strong solvation effect. Some of these associates are found connected by unimers into larger aggregates and are able to crystallize when heated. When THF evaporates spontaneously, these loose associates form well-developed 10 nm lamellar crystals that pack into spherulites.

In slightly selective solvents, both loose and closed micelles are obtained. In benzene, a slightly PS-selective solvent at ∼20 °C, loose micelles coexist with unimers at relatively high concentrations. Closed micelles with crystalline cores are obtained in more diluted (e.g., 0.1%) benzene solutions.

Slightly selective solvents were also created by using neutral/selective solvent mixtures. Addition of CS_2 into THF and benzene solutions successfully makes the solvents more selective. In CS_2/THF mixtures, nanorods are obtained. These nanorods are open so that they crystallized at expense of neighboring copolymer when heated. Polydisperse aggregates formed with addition of CS_2 into the benzene solutions in which loose spherical micelles formed. Spherical, ellipsoidal, and cylindrical micelles are simultaneously observed. Similar structures have been reported in the literature. Judging from the phase images, it seems that they are loose due to the swelling effect of benzene.

It is interesting to find that lamellar micelles with crystalline cores were obtained by addition of CS_2 into 0.1% benzene solutions. Both single-layer and bilayer platelets are observed. These platelet structures are in good accordance with those theoretically predicted and experimentally demonstrated. The bilayer structures are aggregates of single layers associated by very weak van der Waals interactions between the coil coronae.

The lamellar thickness is about 8 nm, much smaller than the coronae thickness provided that the PS blocks are swollen as ideal Gaussian coils with R_g of ∼3 nm. A collapsed conformation of the PS coronae is hypothesized by considering the surface confinement and the

requirement of decreasing the surface energy by covering the crystal core with low-surface-energy PS blocks. Accordingly, the crystal core should be thinner than 3 nm.

Our results provide an overall investigation on the effects of solvent selectivity, from neutral to slightly selective and selective, on the self-assembly of the crystalline−coil diblock copolymers. It seems that, in neutral solvents, the microphase separation of the blocks can slightly shift with concentration due to the varying of polymer−solvent interaction parameters. In slightly selective and selective solvents, the free energy between the micelle core and the solvent dominates, while the crystallization and solvation effect may sometimes contribute.

Acknowledgment. This work is subsidized by the National Natural Science Foundation of China (50125311, 20334010, 20274050, 50390090, 50373041), the Ministry of Science and Technology of China (2003CB615601, 2002CCAD4000), and the Chinese Academy of Sciences (Distinguished Talents Program, KJCX2-SW-H07, KGCX2-205-03).

References and Notes

(1) Hamley, I. W. *The Physics of Block Copolymers*; Oxford University Press: Oxford, 1998.
(2) Förster, S.; Antonietti, M. *Adv. Mater.* **1998**, *10*, 195.
(3) Riess, G. *Prog. Polym. Sci.* **2003**, *28*, 1107.
(4) (a) Ding, J.; Carver, J.; Windle, A. H. *Comput. Theor. Polym. Sci.* **2001**, *11*, 483. (b) Svenson, M.; Alexandridis, P.; Linse, P. *Macromolecules* **1999**, *32*, 637. (c) Pépin, M. P.; Whitmore, M. D. *Macromolecules* **2000**, *33*, 8644. (d) Kim, S. H.; Jo, W. H. *Macromolecules* **2001**, *34*, 7210. (e) Huang, C.-I.; Lodge, T. P. *Macromolecules* **1998**, *31*, 3556.
(5) Utiyama, H.; Takenaka, K.; Mizumori, M.; Fukuda, M.; Tsunashima, Y.; Kurata, M. *Macromolecules* **1974**, *7*, 515.
(6) Zhou, Z.; Chu, B. *Macromolecules* **1988**, *21*, 2548.
(7) Cogan, K.; Gast, A. P. *Macromolecules* **1990**, *23*, 745.
(8) Xu, R.; Winnik, M. A.; Hallett, F. R.; Riess, G.; Croucher, M. D. *Macromolecules* **1991**, *24*, 87.
(9) Antonietti, M.; Heinz, S.; Schmidt, M.; Rosenauer, C. *Macromolecules* **1994**, *27*, 3276.
(10) Tsunashima, Y.; Suzuki, S. *J. Phys. Chem. B* **1999**, *103*, 8675.
(11) Quintana, J. R.; Hernáez, E.; Inchausti, I.; Katime, I. *J. Phys. Chem. B* **2000**, *104*, 1439.
(12) Alexandridis, P.; Yang, L. *Macromolecules* **2000**, *33*, 5574.
(13) Perdersen, J. S.; Hamley, I. W.; Ryu, C. Y.; Lodge, T. P. *Macromolecules* **2000**, *33*, 542.
(14) Lin, E. K.; Gast, A. P. *Macromolecules* **1996**, *29*, 4432.
(15) Ritcher, D.; Schneiders, D.; Monkenbusch, M.; Willner, L.; Fetters, L. J.; Huang, J. S.; Lin, M.; Mortensen, K.; Farago, B. *Macromolecules* **1997**, *30*, 1053.
(16) Ramzi, A.; Prager, M.; Ritcher, D.; Efstratiadis, V.; Hadjichristidis, N.; Young, R. N.; Allgaier, J. B. *Macromolecules* **1997**, *30*, 7171.
(17) Zhang, L.; Eisenberg, A. *J. Am. Chem. Soc.* **1996**, *118*, 3168.
(18) Massey, J.; Power, K. N.; Manners, I.; Winnik, M. A. *J. Am. Chem. Soc.* **1998**, *120*, 9533.
(19) Massey, J. A.; Temple, K.; Cao, L.; Rharbi, Y.; Raez, J.; Winnik, M. A.; Manners, I. *J. Am. Chem. Soc.* **2000**, *122*, 11577.
(20) (a) Raez, J.; Manners, I.; Winnik, M. A. *J. Am. Chem. Soc.* **2002**, *124*, 10381. (b) Raez, J.; Manners, I.; Winnik, M. A. *Langmuir* **2002**, *18*, 7229. (c) Wang, X. S.; Winnik, M. A.; Manners, I. *Macromolecules* **2002**, *35*, 9146.
(21) Vilgis, T.; Halperin, A. *Macromolecules* **1991**, *24*, 2090.
(22) (a) Huang, C.-I.; Chapman, B. R.; Lodge, T. P.; Balsara, N. P. *Macromolecules* **1998**, *31*, 9384. (b) Hanley, K. J.; Lodge, T. P.; Huang, C.-I *Macromolecules* **2000**, *33*, 5918.
(23) Lodge, T. P.; Hamersky, M. W.; Hanley, K. J.; Huang, C.-I. *Macromolecules* **1997**, *30*, 6139.
(24) Lodge, T. P.; Xu, X.; Ryu, C. Y.; Hamley, I. W.; Fairclough, J. P. A.; Ryan, A. J.; Pedersen, J. S. *Macromolecules* **1996**, *29*, 5955.
(25) Lodge, T. P.; Hanley, K. J.; Pudil, B.; Alahapperuma, V. *Macromolecules* **2003**, *36*, 816.
(26) Tao, L.; Luan, B.; Pan, C. Y. *Polymer* **2003**, *44*, 1013.
(27) Zalusky, A. S.; Olayo-Valles, R.; Wolf, J. H.; Hillmyer, M. A. *J. Am. Chem. Soc.* **2002**, *124*, 12716.
(28) Mark, J. E. *Polymer Data Handbook;* Oxford University Press: New York, 1999.
(29) Kubies, D.; Rypáček, F.; Kovářová, J.; Lednický, F. *Biomaterials* **2000**, *21*, 529−536.
(30) Brandrup, J., Immergut, E. H., Grulke, E. A., Abe, A., Bloch, D. R., Eds.; *Polymer Handbook*, 4th ed.; John-Wiley & Sons: New York, 1999.
(31) Jiang, Q.; Shi, H. X.; Li, J. C. *Thin Solid Films* **1999**, *354*, 283.
(32) Zhang, F.; Chen, Y.; Huang, H.; Hu, Z.; He, T. *Langmuir* **2003**, *19*, 5563.
(33) Magonov, S. N.; Reneker, D. H. *Annu. Rev. Mater. Sci.* **1997**, *27*, 175.
(34) Helfand, E.; Tagami, Y. *J. Chem. Phys.* **1972**, *56*, 3592.
(35) (a) Choucair, A.; Eisenberg, A. *Eur. Phys. J. E* **2003**, *10*, 37. (b) Zhang, L.; Eisenberg, A. *Science* **1995**, *268*, 1728. (c) Shen, H.; Eisenberg, A. *Macromolecules* **2000**, *33*, 2561.
(36) Jenekhe, S. A.; Chen, X. L. *Science* **1999**, *283*, 372.
(37) Pitsikalis, M.; Siakali-Kioulafa, E.; Hadjichristidis, N. *Macromolecules* **2000**, *33*, 5460.
(38) (a) Peters, R. D.; Yang, X. M.; Kim, T. K.; Sohn, B. H.; Nealey, P. F. *Langmuir* **2000**, *16*, 4625. (b) Limary, R.; Green, P. F. *Macromolecules* **1999**, *32*, 8167.
(39) Kalb, B.; Pennings, A. J. *Polymer* **1980**, *21*, 607.
(40) Kikkawa, Y.; Abe, H.; Iwata, T.; Inoue, Y.; Doi, Y. *Biomacromolecules* **2001**, *2*, 940.
(41) Brown, H. R.; Russell, T. P. *Macromolecules* **1996**, *29*, 798.

MA035447H